

# The Geometry of Ciliary Dynamics

Mark A. Peterson

*Mount Holyoke College\**

(Dated: May 20, 2009)

## Abstract

Cilia are motile biological appendages that are driven to bend by internal shear stresses between tubulin filaments. A continuum model of ciliary material is constructed that incorporates the essential ciliary constraints: (1) one-dimensional inextensibility of filaments, (2) three-dimensional incompressibility, and (3) shear strain only longitudinally along filaments. It is shown that twist of filaments about each other is not an independent degree of freedom under ciliary constraints. The constraint on twist appears in the equations of motion for cilia as a term not previously recognized. As another application of the same geometrical idea, a general approach to the polymorphism of bacterial flagellae is proposed.

PACS numbers: 45.10.Na, 46.70.Hg, 47.63.Gd

Keywords:

---

\*Electronic address: [mpeterso@mtholyoke.edu](mailto:mpeterso@mtholyoke.edu)

## I. INTRODUCTION

The beating of cilia, or eukaryotic flagella, has been the subject of research for over fifty years. The hydrodynamics of propulsion is one aspect of these studies, concerned with Stokes flows past the cilium at a mesoscale of microns, where the cilium is considered a plane curve or space curve moving in a prescribed way [1][2][3][4] [5][6][7]. The length scale is set by the length of the cilium, with the small diameter of the cilium serving only as a cutoff in the logarithmic singularity of the hydrodynamics.

Another focus of cilia research has been the mechanism by which the cilium generates motion, concerned with the dynein-mediated sliding of microtubule doublets on each other at a nanoscale of tens of nanometers [8] [9][10][11][12][13]. The length scale is set by the diameter of the cilium or even by the size of the motor proteins.

The standard ciliary model, motivated by the structure of the cilium, or axoneme, is called the sliding filament model. The axoneme structure is shown schematically in Fig. 1. There are 9 microtubule doublets around the outside, and 2 in the center. Other components are also visible in electron micrographs: radial spokes connecting the outer microtubules to the central ones, and dynein arms, the motor protein for the system, positioned to walk along adjacent microtubule doublets and generate shear stress between them.

In the sliding filament model the microtubule doublets (the ‘filaments’) are made to slide along each other by the dynein motors. Because shear strain is tightly coupled to bending, the cilium bends, and thus moves. The tight coupling between shear strain and bend, essential for this mechanism, is always assumed either explicitly or implicitly in the form of *ciliary constraints*: (1) the filaments are inextensible, (2) the material is incompressible in the 3-dimensional sense, and (3) shear strain is longitudinal along filaments. In this paper I make these constraints precise in a hypothetical continuum model of “ciliary material,” abstracted from the structure of the axoneme, and I deduce the consequences for the possible states and motion of this material, independent of all other details. Some of these consequences have not been recognized before. I summarize the results in this introductory section.

The ciliary constraints couple shear strain and bend so tightly that it is possible to take as the basic kinematic variables not the shape of the cilium, as is usually done, with equations of motion for that shape, but rather the two independent components of shear strain. This choice is well adapted to modeling the molecular mechanism of ciliary motion, since local

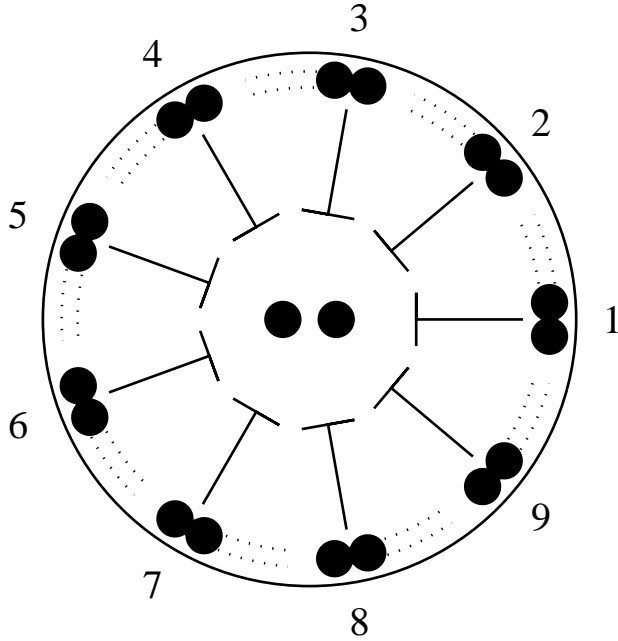


FIG. 1: Schematic cross-section of a cilium showing the 9+2 arrangement of microtubules (dots) and microtubule doublets (double dots), the radial spokes (solid) and the dynein arms (dotted).

strain at the nanoscale knows very little about the largely irrelevant mesoscopic shape of the cilium. The cilium shape is implicit in the state of the shear strain, and can be found from the shear strain by integration, but it is irrelevant for the dynamics (unless one includes the non-local part of the hydrodynamic interaction, which is mesoscopic, and does depend on shape, but is well understood, a separate issue).

The ciliary constraints constrain the twist degree of freedom, i.e. differential rotation about a given filament (differential rotation about the central microtubules of the axoneme, for example). Thus twist is not an independent degree of freedom in ciliary matter. What the ciliary constraints mean for the 9+2 axoneme is illustrated in Fig. 2. Twist has been treated somewhat inconsistently in the past. Twist was not an issue as long as the cilium was modelled as a curve with negligible thickness, so until recently equations of motion just ignored it. More recently, in work of Gueron and Levit-Gurevich [6] and Hilfinger and Jülicher [15], twist is a degree of freedom on a par with other ones. If the ciliary constraints are obeyed (more on this in a moment!), neither of these approaches is quite right. Ciliary matter does twist, and its equations of motion contain terms reflecting this, but these terms involve a Lagrange multiplier, not recognized before, enforcing the ciliary constraints. Thus the ciliary equations of motion incorporating the generally accepted ciliary constraints are derived here in their complete form for the first time.

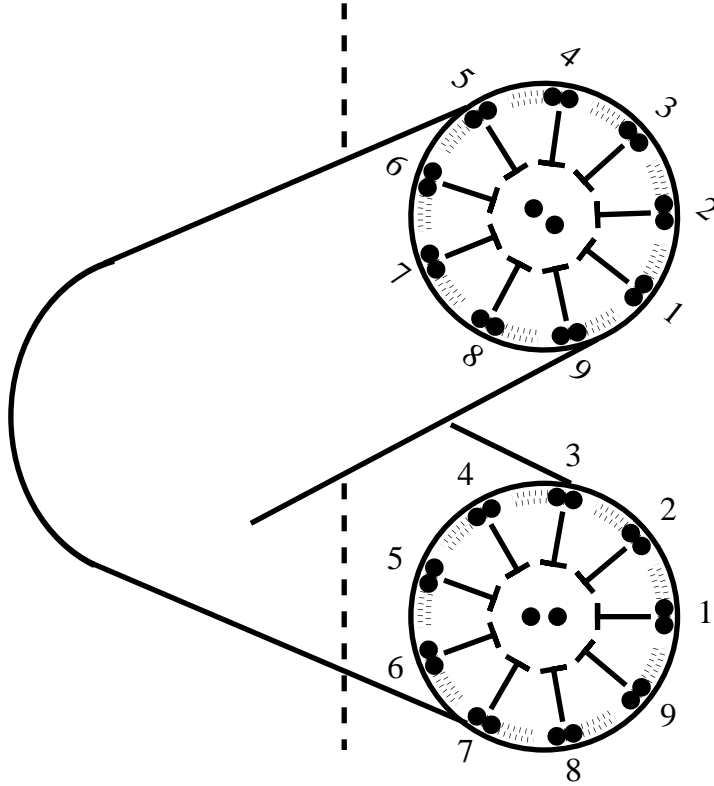


FIG. 2: Under the ciliary constraints, the filaments in the neighborhood of a given filament twist about it in a way that is determined by the geometry of the given filament as a space curve (the displacement vector between the filaments is parallel transported along the given filament). The above 9+2 cilium, which is assumed to have taken a helical shape with curvature  $\kappa = 1$  and torsion  $\tau = 2$ , is shown in cross-section as it intersects a plane containing the helix axis. It twists by about  $38^\circ$  on each turn.

The ciliary constraints forbid the kind of motion shown in Fig. 3, in which initially straight filaments forming a cylinder slide along each other (non-zero shear strain) in order to spiral about the cylinder, but without bending the cylinder. From an evolutionary point of view it is clear that a motile organism depending on its cilia for propulsion would not want this decoupling of shear and bend to happen. It would want to control twist in order to control the orientation of the ciliary beat in space. The ciliary constraints accomplish that. Hilfinger and Jülicher in [15] nonetheless argue that twist is an independent degree of freedom in at least some cilia. Now it turns out that these are not 9+2 cilia, but 9+0 cilia, lacking the central microtubules. They are motile, but their purpose is not to propel an organism but rather to drive a flow with a definite chirality. (Other 9+0 cilia are not

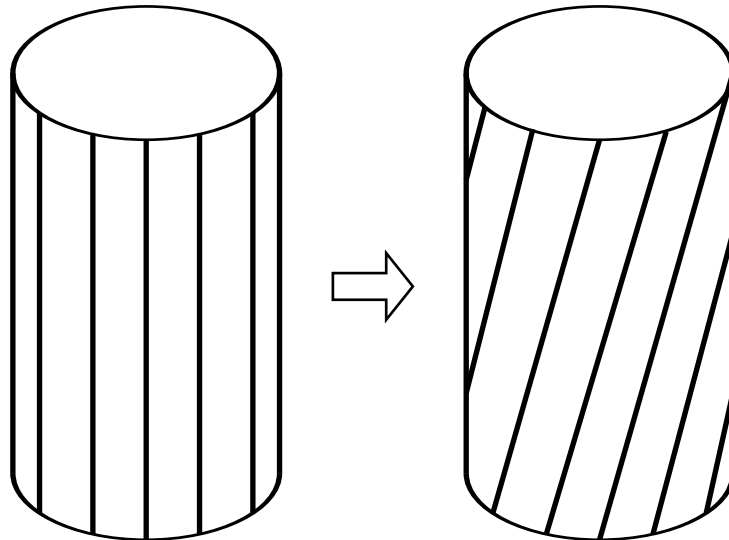


FIG. 3: In a twist transition the microtubules shear along each other, but do not generate bend, i.e., the cylinder remains straight. Such a motion violates the ciliary constraints. It may be possible in a 9+0 axoneme, lacking the central 2 microtubules, but not in a 9+2 axoneme, in which the central microtubules enforce the ciliary constraints. The center of the cylinder is deliberately shown empty here.

even motile.) Apparently the cilia of [15] had to lose the central microtubules to be able to adopt a spiral handedness, as if the central microtubules would have enforced the ciliary constraints that these cilia violate. With a little more insight into the meaning of the ciliary constraints we can see intuitively why the ciliary constraints forbid the motion of Fig 3. As I will show, the ciliary constraints require neighboring filaments to be as parallel as possible, given that they also bend. In the motion of Fig. 3 the outer filaments cannot remain parallel to the central ones, if central ones exist. But if there is nothing in the center, there is nothing there to be parallel to. Perhaps the radial spokes are structures in 9+2 cilia whose purpose is precisely to enforce the ciliary constraints in propulsive cilia for the control of twist.

Because ciliary matter is an abstract model, characterized just by certain constraints and no other stipulations, it might apply to other dense assemblages of filaments than the axonemal structure that suggested it. In a final section I consider what ciliary constraints would mean for the protofilaments of the prokaryotic flagellum and the question of its typically helical shape. Without answering that question I do reduce it to a definite question about strain in a certain surface, assuming ciliary constraints. Remarkably, there might be

an analogue of the 9+2 versus 9+0 phenomenon in the prokaryotic world.

The plan of the paper is as follows. Section II gives an abstract characterization of the three dimensional material that I call ‘ciliary material,’ made up of ‘filaments’ subject to the constraints of the sliding filament model: incompressible, inextensible along the filaments, and admitting shear strain only longitudinally along the filaments. This is an attempt to capture, in a continuum model, the material properties of the cilium. The unexpected result for the states of this material is that one filament can take any shape as a space curve, and all the rest are determined by that one.

Section III determines how the ciliary material can move, subject to its constraints, what I call ciliary flow (note: not the flow driven in the surrounding aqueous medium by a beating cilium, but the motion of the three dimensional ciliary material itself, thought of as a kind of liquid crystal). Consistent with the result of the preceding section, its motion is parameterized by the motion of any single one-dimensional filament, and this one filament can move arbitrarily. Thus the hypothetical ciliary material, motivated by the structure of cilia, combines, in an unexpected way, three-dimensional and one-dimensional properties.

Section IV derives the equation of motion of ciliary material from standard assumptions of continuum mechanics. It turns out to be the usual equation of motion of cilia but with a new term that enforces the constraint on twist. The result is remarkable because the continuum mechanics assumptions say nothing about the cilia shape, and do not even refer to it.

Section V investigates what the ciliary constraints would mean for the material of bacterial flagellae. There are hints that this material may also obey ciliary constraints.

The geometrical methods in Sections II and III are well described in the physics textbooks by Schutz [16] and Frankel [17] for any reader not familiar with them.

## II. CILIARY MATERIAL

In terms of smooth coordinates  $(x^1, x^2, x^3)$  in space one can describe the deformation of any material by the trajectories of its constituent particles, solutions of equations of motion

$$\frac{dx^i}{dt} = V^i(x, t) \tag{1}$$

where

$$V = V^i \partial_i \quad (2)$$

is the velocity vector field, and  $t$  is time. Metric relations among particles are given by

$$ds^2 = g_{ij} dx^i dx^j \quad (3)$$

where  $g_{ij}$  is the Euclidean metric. Coordinatize the material object by Lagrangian coordinates convected by the flow, i.e., let every material point keep the same coordinates that it had originally. The changing metric relationship of material points is then expressed entirely by the change in the metric components  $g_{ij}$ , and the rate of change is given by the Lie derivative

$$\frac{\partial g_{jk}}{\partial t} = V g_{jk} + g([\partial_j, V], \partial_k) + g(\partial_j, [\partial_k, V]) \quad (4)$$

Here  $[\ , \ ]$  is the Lie bracket of vector fields.

As an example of such a computation, let  $V$  be the shearing flow

$$V = yS\partial_x \quad (5)$$

in the plane, where  $S$  is a constant. Then if  $x$  and  $y$  are initially Cartesian coordinates, the metric tensor in convected coordinates at time  $t$  is given by the Lie-Taylor series (which terminates in this case)

$$g + t\mathcal{L}_V g + \frac{t^2}{2!}\mathcal{L}_V \mathcal{L}_V g = \begin{pmatrix} 1 & tS \\ tS & 1 + t^2 S^2 \end{pmatrix}, \quad (6)$$

and evaluating at  $t = 1$  one has the Euclidean metric

$$g = \begin{pmatrix} 1 & S \\ S & 1 + S^2 \end{pmatrix}, \quad (7)$$

in skew coordinates corresponding to constant shear strain  $S$  as shown in Fig. 4.

The flow  $V$  of Eq. (5) is an example of a ciliary flow, and the form of the metric tensor  $g$  in Eq. (7) encodes the result. The filaments, parallel to the  $x$ -axis and labeled by the  $y$  coordinate, slide on each other inextensibly, as one sees in the metric component  $g_{11} = 1$ . The resulting shear strain is visible in the off-diagonal component  $g_{12} = S$ . Finally,  $\det g = 1$  means that the flow is incompressible. The three dimensional generalization of this form to

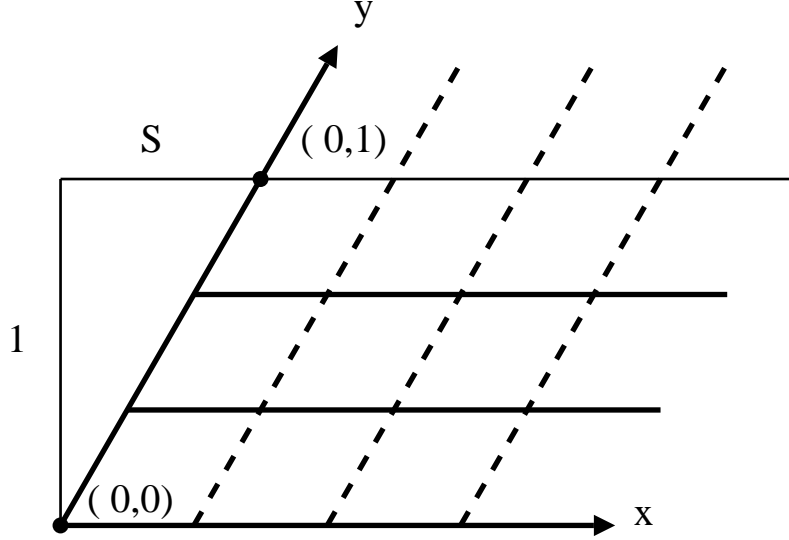


FIG. 4: In the skew coordinates  $(x,y)$  the distance between  $(0,0)$  and  $(0,1)$  is correctly given as  $\sqrt{1+S^2}$  by the metric tensor of Eq. (7) .

a general ciliary configuration is

$$g = \begin{pmatrix} 1 & S & T \\ S & 1+S^2 & ST \\ T & ST & 1+T^2 \end{pmatrix}. \quad (8)$$

where now  $S$  and  $T$ , two independent components of shear strain, depend on Lagrangian coordinates  $(x, y, z)$ . Here  $x$  is arclength along filaments, up to an additive constant reflecting the arbitrariness of choosing an origin in each filament, and the coordinates  $(y, z)$  label the filaments. It should be noted that this is not the most general outcome of an incompressible flow of the filaments, because the only motion that has been allowed to them is sliding longitudinally along each other (and of course bending). These are exactly the constraints of the sliding filament model, encoded in the form of  $g$ . The precise statement of the ciliary constraints is that the metric tensor should have this form in Lagrangian coordinates, which is really a stipulation of the form of the strain.

Associated with the metric tensor  $g$  is an orthonormal frame field

$$e_1 = \partial_x \quad (9)$$

$$e_2 = \partial_y - S\partial_x \quad (10)$$

$$e_3 = \partial_z - T\partial_x. \quad (11)$$

where  $e_1$  is everywhere tangent to filaments. This is not, however, a coordinate frame, because the vector fields do not commute as differential operators, in general.

The metric  $g$  determines the shape of each filament up to a rigid motion, because for each  $(y, z)$  it determines the filament's curvature  $\kappa$  and torsion  $\tau$  as a function of  $x$  (see Appendix A). These are the Frenet data for the filament as a space curve. One has

$$\kappa = \sqrt{S_x^2 + T_x^2} \quad (12)$$

$$\tau = \frac{T_{xx}S_x - S_{xx}T_x}{\kappa^2} \quad (13)$$

where the subscript  $x$  denotes the derivative  $\partial_x$  along the filament. The Frenet equations then determine the filaments as space curves  $\vec{R}(x)$  along with an orthonormal frame  $\{\hat{T}, \hat{N}, \hat{B}\}$  at each point of each curve according to

$$\vec{R}_x = \hat{T} \quad (14)$$

$$\hat{T}_x = \kappa \hat{N} \quad (15)$$

$$\hat{N}_x = -\kappa \hat{T} + \tau \hat{B} \quad (16)$$

$$\hat{B}_x = -\tau \hat{N} \quad (17)$$

In the context of ciliary geometry it is more natural to describe the filaments in terms of the shear strains  $S$  and  $T$  directly than to translate them into the Frenet language. This is an alternative, equivalent description of space curves. It is even possible to translate the other way, from the Frenet description to the ciliary description, inverting the relations in Eqs. (12)-(13),

$$S_x = \kappa \cos \phi \quad (18)$$

$$T_x = \kappa \sin \phi \quad (19)$$

$$\phi_x = \tau \quad (20)$$

In this formulation the space curves  $\vec{R}(x)$  are the solutions of

$$\vec{R}_x = e_1 \quad (21)$$

$$\partial_x e_1 = \kappa \cos \phi e_2 + \kappa \sin \phi e_3 \quad (22)$$

$$\partial_x e_2 = -\kappa \cos \phi e_1 \quad (23)$$

$$\partial_x e_3 = -\kappa \sin \phi e_1 \quad (24)$$

$$\phi_x = \tau \quad (25)$$

There is an arbitrary constant in the angle  $\phi$  since, unlike  $\hat{N}$  and  $\hat{B}$  in the Frenet picture,  $e_2$  and  $e_3$  are only determined up to a global rotation about  $e_1$ . This amounts to a gauge freedom in the ciliary description. An advantage of the ciliary description is that it remains well defined where the curvature vanishes, a nuisance in the Frenet description. These equations imply that the displacement vector from a given filament toward a neighboring filament,  $e_2$  for example, is parallel transported along the given filament. In more physical language, the neighboring filament is as parallel as it can be to the given filament.

The shear strains  $S$  and  $T$  cannot be arbitrary functions, because  $g$  is the Euclidean metric, even if it is expressed in peculiar coordinates. Its associated Riemannian curvature tensor must therefore vanish identically, and hence  $S$  and  $T$  must obey the following identities (see Appendix B)

$$0 = \partial_x(e_2S) = \partial_x(e_3S) = \partial_x(e_2T) = \partial_x(e_3T) \quad (26)$$

$$0 = e_3S - e_2T. \quad (27)$$

The second of these equations can be recognized as

$$[e_2, e_3] = 0. \quad (28)$$

This says that  $e_2$  and  $e_3$  together form an integrable distribution, and thus there exist surfaces normal to the filaments, at least locally. Moreover, since  $e_2$  and  $e_3$  are now an orthonormal coordinate frame field on these surfaces, they are isometric to Euclidean planes. A computation shows that their second fundamental form vanishes ( $[e_2, e_1]$  and  $[e_3, e_1]$  are orthogonal to  $e_2$  and  $e_3$ ). Thus they are not just isometric to Euclidean planes, they actually *are* Euclidean planes, and I will call them normal planes.

By allowing the filaments to reptate along their length inextensibly, one can bring Eq. (26) to the simpler form

$$0 = e_2S = e_3S = e_2T = e_3T \quad (29)$$

that is, the strains  $S$  and  $T$  can be made *constant* in normal planes, as in Fig. 5. Thus the configuration of filaments in a neighborhood of a given filament is entirely determined by that filament. The given filament determines the direction of neighboring filaments, since it determines the normal planes, and it determines their curvatures and torsions, since it determines the values of  $S$  and  $T$ . The geometrical meaning of Eqs. (26)-(27) is that these

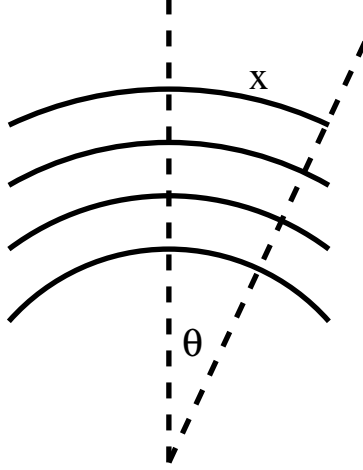


FIG. 5: If filaments are bent into arcs of circles, with arclength  $x$  along the filaments and plane polar coordinates  $(r, \theta)$ , then  $x = r\theta$ , and hence shear strain  $S = -\partial x/\partial r = -\theta = -x/r$  is constant on lines perpendicular to the filaments, a special case of Eq. (29). Also note  $S_x = -1/r$  is the curvature, a special case of Eq. (18). The minus sign is because the curvature vector is opposite to  $e_2 = \partial/\partial r$ .

two potentially conflicting descriptions are consistent. Thus the ciliary geometry is almost rigid. The freedom that it possesses corresponds essentially to a single free space curve.

I turn now to the motions possible in ciliary matter, ciliary flows (note: not flows external to a cilium, but flows within the cilium). Since one of those motions is reptation of filaments, I will also justify the assertions of the preceding paragraph.

### III. CILIARY FLOWS

A ciliary flow, by definition, must maintain the form of Eq. (8) even as  $g$  evolves according to Eq. (4). If  $V$  is the flow with components  $(\alpha, \beta, \gamma)$ , namely

$$V = \alpha\partial_x + \beta\partial_y + \gamma\partial_z, \quad (30)$$

then for  $V$  to be ciliary  $(\alpha, \beta, \gamma)$  must obey the conditions (see Appendix C)

$$0 = \alpha_x + S\beta_x + T\gamma_x \quad (31)$$

$$0 = e_2\beta \quad (32)$$

$$0 = e_3\gamma \quad (33)$$

$$0 = e_2\gamma + e_3\beta \quad (34)$$

$$0 = (e_2\gamma)_x - \beta_x T_x + \gamma_x S_x \quad (35)$$

$$0 = e_2 e_2 \gamma \quad (36)$$

$$0 = e_3 e_3 \beta \quad (37)$$

where the partial derivative  $\partial_x$  is indicated by the subscript  $x$ . Eqs. (36)-(37) are not independent of the others, since for example  $e_3 e_3 \beta = -e_3 e_2 \gamma = -e_2 e_3 \gamma = 0$ . In fact all higher derivatives of  $\beta$  and  $\gamma$  in the normal planes vanish by this argument, so that  $\beta$  and  $\gamma$  restricted to a normal plane can only be affine linear functions. I return to this consideration below.

The simplest nontrivial ciliary flow is reptation,  $\alpha_x = \beta = \gamma = 0$ . By Eq. (4) the shear strains change under this flow at the rate

$$S_t = \alpha_y + \alpha S_x \quad (38)$$

$$T_t = \alpha_z + \alpha T_x, \quad (39)$$

where subscripts indicate partial derivatives with respect to the corresponding variable. It is possible to construct a reptation  $\alpha$  that alters  $S$  and  $T$  in such a way that Eq. (29) holds in one normal plane, at least locally (see Appendix D). Then by Eq. (26)  $S$  and  $T$  are constant in every normal plane along the filaments. This proves the assertions made at the end of the last section. I will now assume that  $S$  and  $T$  obey the simpler Eq. (29), since this can always be arranged by a reptation.

The ciliary conditions require  $\beta$  and  $\gamma$  to be affine linear functions in the normal planes. To see that there exist non-trivial solutions to these conditions, imagine specifying  $\beta(x)$  and  $\gamma(x)$  arbitrarily along one filament. Integrating Eq. (35) determines  $e_2\gamma = -e_3\beta$  along the filament up to an arbitrary global constant. These are all the data required to extend  $\beta$  and  $\gamma$  in each normal plane as affine linear functions. This extension continues to satisfy Eq. (35) on neighboring filaments because of the easily verified identities

$$e_2[(e_2\gamma)_x - T_x\beta_x + S_x\gamma_x] = 2S_x[(e_2\gamma)_x - T_x\beta_x + S_x\gamma_x] \quad (40)$$

$$e_3[(e_2\gamma)_x - T_x\beta_x + S_x\gamma_x] = 2T_x[(e_2\gamma)_x - T_x\beta_x + S_x\gamma_x] \quad (41)$$

Repeated differentiation of Eq. (35) using  $e_2$  and  $e_3$  shows that if  $(e_2\gamma)_x - T_x\beta_x + S_x\gamma_x$  vanishes on a filament, then all its normal derivatives also vanish there. Thus given only

that it is represented by its Taylor series, it is constant, and hence zero, and the constructed solution obeys all the ciliary conditions.  $V$  is a non-trivial ciliary flow, determined by its values on one filament.

The conditions Eqs. (31)-(37) confirm that the ciliary configuration is entirely determined by one filament. If one tries to move the filaments, one can specify  $\beta(x)$  and  $\gamma(x)$  on only one given filament. The ciliary conditions then determine  $\alpha(x)$  along that filament up to a constant (a reptation). They further determine  $\beta$  and  $\gamma$  almost uniquely as linear functions in normal planes. Neighboring filaments intersect the normal planes (each plane labelled by  $x$ , its intersection with the given filament), and in the course of the motion these intersection points rotate about the given filament at an angular velocity

$$\omega(x) = (e_2\gamma)(x) \quad (42)$$

which is not arbitrary but is determined up to a global constant by  $\beta$  and  $\gamma$  according to Eq. (35). (The undetermined constant in  $\omega$  describes a global twisting rotation in which every normal plane rotates at the same rate, a motion which is possible but probably not physically relevant.) The remaining freedom in  $\alpha$  corresponds to reptations of neighboring filaments. Thus, to summarize, any filament determines the configurations of its neighbors, and any motion of that filament determines the motion of its neighbors. It is worth noting what was not obvious *a priori*, that non-trivial motions of the filaments are possible, that is, the ciliary material is not completely rigid. One filament can move arbitrarily (but inextensibly), and all the others must follow it.

#### IV. CILIARY DYNAMICS

I now model the dynamics of the cilium by applying standard ideas of continuum mechanics to a thin cylinder of ciliary matter of length  $L$  and radius  $\rho$ , all dynamical quantities depending just on  $x$ , the coordinate along one given filament. That filament can of course have any shape, so the cylinder is not necessarily straight. Let the cilium have elastic moduli, so that the energy of a configuration is given by the shear energy and bending energy

$$E = \frac{\mu}{2} \int_0^L [(S - F)^2 + (T - G)^2] dx + \frac{\kappa_c}{2} \int_0^L (S_x^2 + T_x^2) dx, \quad (43)$$

where  $\mu$  is the shear modulus and  $\kappa_c$  is the bending modulus (with dimensions appropriate to one dimension, not three). Here  $F$  and  $G$  are target shear strains, such that the shear

energy would be minimal if the shear strains  $S$  and  $T$  could relax to  $F$  and  $G$ . The operation of the ciliary “engine” would be to make  $F$  and  $G$  functions of time, so that the equilibrium becomes a moving target. Asymmetries in the nanoscopic structure of the cilium could be built into this expression, which is taken symmetrical here for illustration.

Conjugate to shear strains  $S$  and  $T$  are internal stresses

$$\Phi = \delta E / \delta S = \mu(S - F) - \kappa_c S_{xx} \quad (44)$$

$$\Psi = \delta E / \delta T = \mu(T - G) - \kappa_c T_{xx} \quad (45)$$

which, by the above mentioned one-dimensionality, have the units of force.

Continuing this variational approach to the dynamics, one finds the generalized forces conjugate to the displacement of a cilium along  $V = \alpha \partial_x + \beta \partial_y + \gamma \partial_z$  of Eq. (30), together with the required rotation  $\omega$  of Eq.(42) in normal planes. In the orthonormal basis,  $V$  takes the form

$$V = (\alpha + \beta S + \gamma T)e_1 + \beta e_2 + \gamma e_3, \quad (46)$$

a representation that becomes increasingly appropriate as one moves up to the mesoscopic scale. Note that  $\beta$  and  $\gamma$  are the components of velocity normal to the cilium, but that they also contribute to the tangential velocity if the shear strains are non-zero. This is a residual piece of three dimensional information in the one-dimensional description of the cilium as a curve.

From Eq. (4), imposing Eqs. (31)-(37), the strains under the flow  $V$  change at the rate

$$S_t = (\alpha + \beta S + \gamma T)S_x + \beta_x + e_2 \alpha + \omega T \quad (47)$$

$$T_t = (\alpha + \beta S + \gamma T)T_x + \gamma_x + e_3 \alpha - \omega S \quad (48)$$

The terms  $e_2 \alpha$  and  $e_3 \alpha$  represent reptations within the cilium, a possibility that is ignored from now on. The constraints

$$0 = \alpha_x + S\beta_x + T\gamma_x \quad (49)$$

$$0 = \omega_x - T_x \beta_x + S_x \gamma_x \quad (50)$$

are handled with Lagrange multipliers  $\lambda$  and  $\nu$  in the expression

$$E' = E + \int_0^L \lambda(\alpha_x + S\beta_x + T\gamma_x) dx + \int_0^L \nu(\omega_x - T_x \beta_x + S_x \gamma_x) dx \quad (51)$$

Then the generalized interior forces on the cilium are

$$F_\alpha = -\delta E' / \delta \alpha = -\Phi S_x - \Psi T_x + \lambda_x \quad (52)$$

$$F_\beta = -\delta E' / \delta \beta = -\Phi S S_x - \Psi S T_x + \Phi_x + (\lambda S)_x - (\nu T_x)_x \quad (53)$$

$$F_\gamma = -\delta E' / \delta \gamma = -\Phi T S_x - \Psi T T_x + \Psi_x + (\lambda T)_x + (\nu S_x)_x \quad (54)$$

$$F_\omega = -\delta E' / \delta \omega = \nu_x - \Phi T + \Psi S \quad (55)$$

Generalized external forces on the cilium, due to the fluid medium of viscosity  $\eta$  in which it is immersed, can be found from the dissipation function  $D$  for the corresponding Stokes flow. A thorough analysis of this problem has been done by Gueron and Liron [4]. For simplicity I take just the leading term indicated by their analysis,

$$D = \int_0^L \left[ \frac{C_T}{2} (\alpha + \beta S + \gamma T)^2 + \frac{C_N}{2} (\beta^2 + \gamma^2) + \frac{C_\omega}{2} \omega^2 \right] dx \quad (56)$$

where the  $C$ 's are constant resistance coefficients. The viscous force conjugate to displacement by  $\alpha$  is then  $-\delta D / \delta \alpha$ , etc. Requiring that elastic forces and viscous forces balance, i.e.,

$$\frac{\delta E'}{\delta \alpha} = \frac{\delta D}{\delta \alpha}, \quad (57)$$

etc., leads to the surprisingly simple dynamical laws connecting the motion of ciliary matter to its internal stresses,

$$C_T(\alpha + \beta S + \gamma T) = -\Phi S_x - \Psi T_x + \lambda_x \quad (58)$$

$$C_N \beta = \Phi_x + \lambda S_x - (\nu T_x)_x \quad (59)$$

$$C_N \gamma = \Psi_x + \lambda T_x + (\nu S_x)_x \quad (60)$$

$$C_\omega \omega = \nu_x - \Phi T + \Psi S \quad (61)$$

Under this flow the strains change according to Eqs. (47)-(48). The Lagrange multipliers can now be determined from the constraints Eqs. (49)-(50). Substituting the solutions in Eqs. (58)-(61) gives the equations for  $\lambda$  and  $\nu$ ,

$$\lambda_{xx} = \frac{C_T}{C_N} \kappa^2 \lambda + (\Phi S_x + \Psi T_x)_x + \frac{C_T}{C_N} (S_x \Phi_x + T_x \Psi_x) + \frac{C_T}{C_N} \tau \kappa^2 \nu \quad (62)$$

$$\nu_{xx} = (\Phi T - \Psi S)_x - \frac{C_\omega}{C_N} \left[ S_x \Psi_{xx} - T_x \Phi_{xx} + \lambda \tau \kappa^2 + T_x (\nu T_x)_{xx} + S_x (\nu S_x)_{xx} \right], \quad (63)$$

where I have used the expressions for curvature  $\kappa$  and torsion  $\tau$  first derived in terms of  $S$  and  $T$  in Eqs. (12)-(13). In the limit as  $C_\omega / C_N \rightarrow 0$ , the equation for  $\nu$  simplifies considerably,

with solution

$$\nu = \int_0^x (\Phi T - \Psi S) dx + c_1 x + c_2 \quad (64)$$

The solution for  $\omega$  is already explicit in terms of  $\beta$  and  $\gamma$  from the constraint Eq. (50),

$$\omega = \int_0^x (T_x \beta_x - S_x \gamma_x) dx + \text{const.} \quad (65)$$

With one important exception, the above dynamical laws for ciliary matter are precisely the usual phenomenological laws for three-dimensional motions of cilia, as derived by Gueron and Liron [5]. It is remarkable that they emerge here without any appeal or reference to the shape of the cilium (apart from the hydrodynamic interaction that one could introduce into a more accurate dissipation function, Eq. (56)), but purely as a consequence of the dynamics of  $S$  and  $T$ . The occurrence of  $\kappa$  and  $\tau$  above is just an abbreviation for certain combinations of derivatives of  $S$  and  $T$  that appeared. Of course the large scale shape of the cilium could be reconstructed at any time from Eqs. (18)-(25).

The dynamical laws have been expressed here in terms of the force vector

$$\vec{F} = \lambda e_1 + \Phi e_2 + \Psi e_3 \quad (66)$$

but the vector quantities in [5] were expressed in terms of the Frenet basis  $\hat{T}, \hat{N}, \hat{B}$ , where  $\vec{F}$  took the form

$$\vec{F} = -F_T \hat{T} - F_N \hat{N} - F_B \hat{B}. \quad (67)$$

From Eqs. (18)-(22) one has the transformation that connects these two descriptions,

$$\hat{T} = e_1 \quad (68)$$

$$\hat{N} = \cos \phi e_2 + \sin \phi e_3 \quad (69)$$

$$\hat{B} = -\sin \phi e_2 + \cos \phi e_3 \quad (70)$$

with  $\phi_x = \tau$ , the torsion of the curve. Using also Eqs. (12)-(13), it is straightforward to verify that the dynamical laws of ciliary matter, as derived here, agree with standard phenomenology in every respect but one: in ciliary matter there is an additional constraint, and a corresponding additional term in the laws.

The additional constraint arises because the sliding filament model is constrained by more than just the inextensibility of the filaments. Its constraints are expressed in the form of the strain tensor, or equivalently in the form of the metric tensor in Lagrangian coordinates,

Eq. (8). It is to be expected that these additional constraints would have consequences for the dynamics, just as inextensibility does, through the Lagrange multiplier  $\lambda$ . The dynamical form that this constraint takes is a certain definite coupling of shear and twist, the last terms in Eqs. (59)-(60), and more generally every reference to the Lagrange multiplier  $\nu$  and the twist velocity  $\omega$ . Models of ciliary dynamics should either include these terms or justify the violation of ciliary constraints.

## V. HELICES AND PROKARYOTIC FLAGELLAE

The flagellae of bacteria are unrelated to the cilia of eukaryotic cells. They are typically helices of well defined curvature and torsion, although within each bacterial species they exhibit polymorphism: more than one helix may exist as a metastable form. The helical flagellum is turned by a rotary motor in the bacterial cell membrane like a screw propeller. This mechanism of cell motility is clearly very different from the sliding filament mechanism that causes cilia to beat.

The structure of the flagellum is nonetheless somewhat reminiscent of that of the cilium. The protein flagellin polymerizes to form protofilaments, and typically 11 protofilaments self-assemble side by side to form a hollow tube that is the flagellum. The protofilaments constituting the flagellum may wrap around its helical form in either the left handed or right handed sense. In a polymorphic transition, everything changes together, and may even change from right handed to left handed, or the reverse. Attempts to understand the existence of the helical form in the first place, and its polymorphism, have continued since pioneering work of S. Asakura[18]. Recent work including a good introduction to the problem is the article of S. Srigiriraju and T. Powers[19].

The behavior described above is not unlike that of ciliary matter. The necessarily cooperative motion of all filaments together, exhibited in the collective behavior of the protofilaments in flagellar polymorphic transitions, is the most characteristic feature of what I have called ciliary flow. And as I show below, if one filament is a helix, the nearby ones wind around it in the manner of the flagellin protofilaments around the centerline of the helical flagellum. These similarities in the properties of abstract ciliary matter and real flagellae motivate the following observations.

Ciliary matter is almost rigid, and there is almost nothing about it that is adjustable.

The only freedom is to choose the shape of one filament. Let that one filament be a helix with curvature  $\kappa$  and torsion  $\tau$ ,

$$X = \frac{\kappa}{\kappa^2 + \tau^2} \cos \sqrt{\kappa^2 + \tau^2} x \quad (71)$$

$$Y = \frac{\kappa}{\kappa^2 + \tau^2} \sin \sqrt{\kappa^2 + \tau^2} x \quad (72)$$

$$Z = \frac{\tau x}{\sqrt{\kappa^2 + \tau^2}}, \quad (73)$$

where  $(X, Y, Z)$  are fixed Cartesian coordinates, and  $x$  is arclength along the helix. Then, integrating Eqs. (18)-(20), the local shear strains between filaments are

$$S = \frac{\kappa}{\tau} \sin \tau x \quad (74)$$

$$T = -\frac{\kappa}{\tau} \cos \tau x. \quad (75)$$

Inverting Eqs. (69)-(70), we see that along this helix the vectors  $e_2$  and  $e_3$  rotate with respect to the Frenet frame with (spatial) period  $2\pi/\tau$ ,

$$e_2 = \cos(\tau x) \hat{N} - \sin(\tau x) \hat{B} \quad (76)$$

$$e_3 = \sin(\tau x) \hat{N} + \cos(\tau x) \hat{B} \quad (77)$$

Since  $e_2$  and  $e_3$  are defined by Lagrangian coordinates, and point to definite filaments, this is not just the behavior of the coordinates, it means that the filaments of the ciliary matter spiral about the central helix in this way, reminiscent of the spiraling of protofilaments in the flagellum, as I noted above.

We are thus motivated to ask whether the protofilaments in the flagellum can be modeled by the filaments of ciliary matter. It is immediate that sometimes the answer is ‘no.’ There is a form of flagellin that forms a straight flagellar filament, i.e., a straight hollow cylinder, in which the protofilaments that make up the cylinder spiral around the cylinder, like the second cylinder in Fig. 3. By the rigidity of ciliary matter, if the protofilaments are helices, then the flagellum itself should be a helix, and if the flagellum is straight, then the protofilaments must be straight, like the first cylinder in Fig 3. Yet it is obvious that a straight cylinder can be made of helical protofilaments, as happens in this case, just as it can presumably happen in the 9+0 cilium [15].

The form of flagellin described above lacks a piece that extends inside the cylinder and forms connections there among the protofilaments into what could be functionally a twelfth,

central protofilament. In Ref. [19] this central component was modeled as a central elastic rod. I consider the possibility that it completes the three-dimensional structure, in the same way that I have conjectured that the central microtubules complete it in the 9+2 cilium and impose the ciliary constraints. With this (normal) flagellin the flagellum does behave more like ciliary matter, as I have already noted. In Ref. [19] elastic stress imposed by the central rod on the outer filaments was necessary to obtain the observed behavior: this may be an equivalent way of saying that the central rod imposes the ciliary constraints.

Within the model of ciliary material it is easy to find the strain tensor in the cylindrical surface of the flagellum, relative to the reference configuration of the straight flagellum, as the flagellum varies through all helical shapes. It is this surface strain, and the associated elastic energy, that is thought to control and select the observed helical shapes of flagella as local elastic energy minima. I have already found in Eqs. (74)-(75) the two independent functions  $S$  and  $T$  in the metric tensor  $g$  along a general helix, which I take to be the centerline of the flagellum. The cylindrical surface surrounding this helix at a distance  $\rho \approx 10$  nm can be coordinatized by  $x$  and  $\theta$ , where  $(\rho, \theta)$  are polar coordinates in normal planes, and the direction of  $e_2$  is  $\theta = 0$ . Note that  $\theta$  is then a Lagrangian coordinate, labelling protofilaments on the surface of the flagellum. In particular,  $\theta = 0$  labels the protofilament pointed to by  $e_2$ . I restrict  $g$  to the surface by evaluating it on  $\partial/\partial x$  and  $\partial/\partial\theta$ , where

$$\frac{\partial}{\partial\theta} = -\rho \sin\theta \frac{\partial}{\partial y} + \rho \cos\theta \frac{\partial}{\partial z}. \quad (78)$$

Ignoring higher order corrections in  $\kappa\rho \lesssim 0.01$ , I find

$$g = \begin{pmatrix} 1 & -(\rho\kappa/\tau) \cos(\tau x - \theta) \\ -(\rho\kappa/\tau) \cos(\tau x - \theta) & \rho^2 [1 + ((\rho\kappa/\tau) \cos(\tau x - \theta))^2] \end{pmatrix} \quad (79)$$

The two-dimensional strain tensor  $U$  is therefore, up to a factor of 2, the difference of this tensor from its value at the reference configuration  $\kappa = 0$ , namely

$$U = \frac{1}{2} \begin{pmatrix} 0 & -(\rho\kappa/\tau) \cos(\tau x - \theta) \\ -(\rho\kappa/\tau) \cos(\tau x - \theta) & ((\rho^2\kappa/\tau) \cos(\tau x - \theta))^2 \end{pmatrix} \quad (80)$$

There is essentially just one independent component of shear strain,

$$U_{x\theta} = -(\rho\kappa/\tau) \cos(\tau x - \theta). \quad (81)$$

The challenge in modelling the flagellum is to understand what is the underlying elastic energy that is minimized, at least locally, by this strain at the observed helical values of  $\kappa$

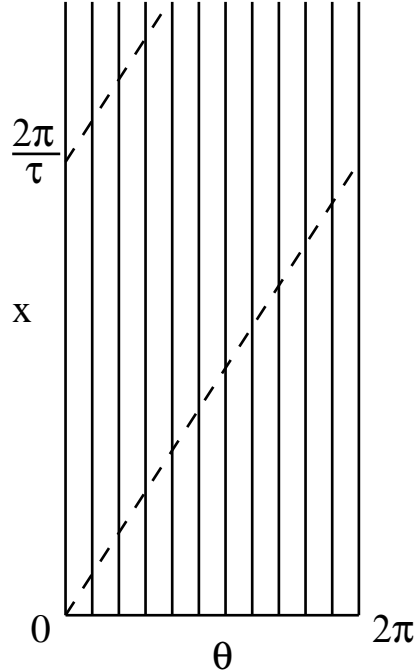


FIG. 6: The coordinate plane for the surface of the flagellum has lines of constant  $\theta$  that map onto spiraling protofilaments. The coordinate  $x$  is arclength along protofilaments. The dotted line is a line of constant shear strain, determining that the flagellum is a helix of torsion  $\tau$ .

and  $\tau$ . Any explanation for why the surface of the flagellum is strained in this way would explain the shape of the prokaryotic flagellum, assuming ciliary constraints.

It is worth noting a point of common sense about this result, illustrated in Fig. 6, which almost could be guessed without any computation. Since any fixed protofilament (fixed  $\theta$ ) spirals around the helical flagellum, the shear strain in its neighborhood must be periodic in  $x$  with period  $2\pi/\tau$ , as it visits the inside of the helix, then the outside, etc. Helical symmetry then requires the strain to have the form of Eq. (81), at least the lowest order Fourier component. Since protofilaments really do spiral around the flagellum, the actual strain in the surface must look like this even if ciliary matter turns out not to be a good model for it.

Detailed models of how strain is introduced into the surface, as the flagellum seeks its equilibrium configuration, suggest that there could be local conformational changes, rotations, or displacements of the flagellin units that make up the protofilaments. In particular, these changes, with their attendant shear strain, could be cooperative within a protofilament[19], propagating shear strain along it. The picture that emerges from the ciliary model is similar,

but not identical to this. If the shear strain were propagated along a protofilament, it would depend on the protofilament (i.e., on  $\theta$ ), but not on  $x$ , which is not the form of Eq. (81). Of course the ultimate shear strain in Eq. (81) could be driven by an imposed strain of a different form, with the flagellum eventually relaxing into Eq. (81) as a compromise involving other elastic energies, but the most straightforward idea is that the above shear strain is simply imposed by whatever the mechanism is. In the language of cooperative interaction between flagellin units, it says that the shear strain propagates along a protofilament, but is gradually also communicated to the neighboring protofilament on one side. The distance required for this strain to visit all protofilaments in turn and return to the original protofilament determines  $\tau$ , the torsion of the eventual flagellum helix, and the maximum amplitude of the shear strain determines  $\kappa$ , the curvature of the eventual helix. In this way nanoscopic details of interaction would determine the mesoscopic form of the flagellum

Pursuing such details here would take me away from the original purpose of this paper, which was to point out useful and previously unrecognized properties of a model that is already widely used in biophysics, a continuum approximation to the sliding filament model.

### Appendix A: Ciliary filaments as space curves

The rates of change of the vector fields  $e_2, e_3$ , along the integral curves of  $e_1$ , (the filaments of the ciliary space) are given by the Lie derivatives (Lie brackets)

$$\partial_x e_2 = [e_1, e_2] = -S_x e_1 \tag{A1}$$

$$\partial_x e_3 = [e_1, e_3] = -T_x e_1 \tag{A2}$$

where the subscript  $x$  indicates  $\partial_x$ , the derivative along a filament. Thus the curvature vector, in the sense of the Frenet equations, is

$$\kappa \hat{N} = S_x e_2 + T_x e_3 \tag{A3}$$

where the curvature is the norm of this vector

$$\kappa = \sqrt{S_x^2 + T_x^2}. \tag{A4}$$

The rate of change of the principal normal  $\hat{N}$  along the filament, dotted with the binormal

$$\hat{B} = \frac{S_x e_3 - T_x e_2}{\kappa} \tag{A5}$$

is the torsion

$$\tau = g([e_1, \hat{N}], \hat{B}) = \frac{T_{xx}S_x - S_{xx}T_x}{\kappa^2} \quad (\text{A6})$$

### Appendix B: Consequences of flat geometry

Differential forms dual to the orthonormal vector fields  $e_1, e_2, e_3$  of Eqs. (9)-(11) are

$$\sigma^1 = dx + Sdy + Tdz \quad (\text{B1})$$

$$\sigma^2 = dy \quad (\text{B2})$$

$$\sigma^3 = dz. \quad (\text{B3})$$

Define

$$A = \frac{1}{2}(TS_x - ST_x + T_y - S_z). \quad (\text{B4})$$

It is straightforward to verify that the connection forms

$$\omega^1_1 = \omega^2_2 = \omega^3_3 = 0 \quad (\text{B5})$$

$$\omega^1_2 = -\omega^2_1 = -S_x\sigma^1 + A\sigma^3 \quad (\text{B6})$$

$$\omega^1_3 = -\omega^3_1 = -T_x\sigma^1 - A\sigma^2 \quad (\text{B7})$$

$$\omega^2_3 = -\omega^3_2 = -A\sigma^1 \quad (\text{B8})$$

satisfy the Cartan structure equations

$$d\sigma^i + \omega^i_j \wedge \sigma^j = 0. \quad (\text{B9})$$

Now because the metric is flat, the curvature forms

$$\theta^i_j = d\omega^i_j + \omega^i_k \wedge \omega^k_j \quad (\text{B10})$$

must vanish identically. In particular,

$$\theta^2_3 = -2A\sigma^2 \wedge \sigma^3 + \text{other components} \quad (\text{B11})$$

so  $A$  must vanish, and this is Eq. (27). The remaining identities reduce to  $d\omega^1_2 = d\omega^1_3 = 0$ , and this is Eq (26).

### Appendix C: Geometrical calculations for ciliary flows

Under a ciliary flow  $V$  it is necessary that  $g_{11}$  keep the constant value 1, so that

$$0 = \partial_t g_{11} = 2g([\partial_x, V], \partial_x) = 2(\alpha_x + S\beta_x + T\gamma_x), \quad (\text{C1})$$

and this is Eq. (31). To preserve the form of  $g$  it is necessary that

$$\partial_t g_{22} = 2SS_t = 2S\partial_t g_{12} \quad (\text{C2})$$

$$\partial_t g_{33} = 2TT_t = 2T\partial_t g_{13} \quad (\text{C3})$$

$$\partial_t g_{23} = ST_t + TS_t = S\partial_t g_{13} + T\partial_t g_{12} \quad (\text{C4})$$

and these conditions, using Eq. (4), are Eqs. (32)-(34). Finally, it is not enough that  $g$  keep the form of Eq. (8), it must also continue to have zero Riemannian curvature. The most efficient way to handle this computation is to use the moving orthonormal frame associated with the changing  $g$ . The change in these vector fields is computed by the Lie derivative (the Lie bracket for vector fields). Thus under the ciliary flow  $V$  of Eq. (30)

$$\partial_t e_1 = [e_1, V] = \alpha_x e_1 + \beta_x \partial_y + \gamma_x \partial_z = \beta_x e_2 + \gamma_x e_3 \quad (\text{C5})$$

$$\partial_t e_2 = [e_2, V] - (\partial_t S)e_1 = (\sigma^1([e_2, V]) - \partial_t S) e_1 + (e_2 \gamma) e_3 \quad (\text{C6})$$

$$\partial_t e_3 = [e_3, V] - (\partial_t T)e_1 = (\sigma^1([e_3, V]) - \partial_t T) e_1 + (e_3 \beta) e_2 \quad (\text{C7})$$

As a check, one verifies what is required by orthonormality,

$$\partial_t S = \sigma^1([e_2, V]) + \beta_x \quad (\text{C8})$$

$$\partial_t T = \sigma^1([e_3, V]) + \gamma_x, \quad (\text{C9})$$

using Eq. (4), and also  $e_3 \beta = -e_2 \gamma$  by Eq. (34). To summarize,

$$\partial_t e_1 = \beta_x e_2 + \gamma_x e_3 \quad (\text{C10})$$

$$\partial_t e_2 = -\beta_x e_1 - (e_3 \beta) e_3 \quad (\text{C11})$$

$$\partial_t e_3 = -\gamma_x e_1 - (e_2 \gamma) e_2 \quad (\text{C12})$$

For the Riemannian curvature to vanish it is necessary that

$$0 = \partial_t [e_2, e_3] = [\partial_t e_2, e_3] + [e_2, \partial_t e_3] \quad (\text{C13})$$

$$= [(e_3 \beta)_x - (e_2 \gamma)_x + 2T_x \beta_x - 2S_x \gamma_x] e_1 + (e_2 e_2 \gamma) e_2 + (e_3 e_3 \beta) e_3 \quad (\text{C14})$$

The vanishing of this vector field is conditions Eqs. (35)-(37). It remains to show that with these conditions the other components of the Riemannian curvature continue to vanish identically. Dual to Eqs. (C10)-(C12) one has

$$\partial_t \sigma^1 = \beta_x \sigma^2 + \gamma_x \sigma^3 \quad (\text{C15})$$

$$\partial_t \sigma^2 = -\beta_x \sigma^1 - (e_3 \beta) \sigma^3 \quad (\text{C16})$$

$$\partial_t \sigma^3 = -\gamma_x \sigma^1 - (e_2 \gamma) \sigma^2 \quad (\text{C17})$$

The Cartan structure equations, which are identities, require

$$\partial_t \omega^1_2 = (-\beta_{xx} + T_x(e_3 \beta)) \sigma^1 - S_x \beta_x \sigma^2 - S_x \gamma_x \sigma^3 \quad (\text{C18})$$

$$\partial_t \omega^1_3 = (-\gamma_{xx} + S_x(e_2 \gamma)) \sigma^1 - T_x \beta_x \sigma^2 - T_x \gamma_x \sigma^3 \quad (\text{C19})$$

$$\partial_t \omega^2_3 = 0 \quad (\text{C20})$$

and a long but straightforward computation then shows that

$$\partial_t (d\omega^i_j + \omega^i_k \wedge \omega^k_j) = 0 \quad (\text{C21})$$

for all components.

#### Appendix D: Making $S$ and $T$ constant in one normal plane by reptation

Let  $\alpha$  be a reptation, i.e.,  $V = \alpha \partial_x$  and  $\alpha_x = 0$ . Then, rearranging Eqs. (38)-(39), the convective derivative

$$S_t - \alpha S_x = \alpha_y \quad (\text{D1})$$

$$T_t - \alpha T_x = \alpha_z \quad (\text{D2})$$

is the rate of change of strain in a fixed normal plane. (The normal planes are not convected with the material but are associated with the stationary pattern of the filaments, so to stay in a normal plane, subtract the convective term). Thus in a fixed normal plane, since  $\alpha_x = 0$ ,

$$(e_2 S)_{t'} = e_2 (S_t - \alpha S_x) = e_2 \alpha_y = e_2 e_2 \alpha \quad (\text{D3})$$

$$(e_3 T)_{t'} = e_3 (T_t - \alpha T_x) = e_3 \alpha_z = e_3 e_3 \alpha \quad (\text{D4})$$

$$(e_3 S)_{t'} = (e_2 T)_{t'} = e_2 e_3 \alpha \quad (\text{D5})$$

Here the subscript  $t'$  means the time derivative at a fixed normal plane, not at fixed  $x$ . In this normal plane, we can introduce coordinates  $(y', z')$  such that  $e_2 = \partial/\partial y'$ ,  $e_3 = \partial/\partial z'$ . Then by the Poincaré lemma, Eq. (27) says that there exists locally a function  $F(y', z', t)$  such that in that plane  $S = e_2 F$ ,  $T = e_3 F$ . Extend  $F$  to be constant along filaments, and take  $\alpha = -F$ . Then under the reptation  $V = \alpha \partial_x$ ,

$$(e_2 S)_{t'} = -e_2 S \tag{D6}$$

$$(e_3 T)_{t'} = -e_3 T \tag{D7}$$

$$(e_3 S)_{t'} = (e_2 T)_{t'} = -e_3 S = -e_2 T. \tag{D8}$$

Thus these quantities decay to zero exponentially with time. In the limit as  $t \rightarrow \infty$ , Eq. (29) holds in one normal plane (and then by Eq. (26) it holds in all normal planes).

- 
- [1] J. Gray and G. Hancock, *J. Exp. Biol.* **32**, 802-814 (1955).
  - [2] J. Lighthill, *Soc. Ind. Appl. Math. Rev.* **18**, 161 (1976).
  - [3] R.E. Johnson and C.J. Brokaw, *Biophys. J.* **25** 113-127 (1979).
  - [4] S. Gueron and N. Liron, *Biophys. J.* **63** 1045-1058 (1992).
  - [5] S. Gueron and N. Liron, *Biophys. J.* **65** 499-507 (1993).
  - [6] S. Gueron and K. Levit-Gurevich, *Mathematical Methods in the Applied Sciences* **24** 1577-1603 (2001).
  - [7] A. Vilfan and F. Jülicher, *Phys. Rev. Lett.* **96** 058102 (2006).
  - [8] C.J. Brokaw, *Biophys. J.* **12** 564-586 (1972).
  - [9] J. Lubliner, *J. Theor. Biol.* **41** 119-125 (1973).
  - [10] M. Hines and J.J. Blum, *Biophys. J.* **23** 41-57 (1978).
  - [11] M. Hines and J.J. Blum, *Biophys. J.* **41** 67-79 (1983).
  - [12] M. Hines and J.J. Blum, *Biophys. J.* **46** 559-565 (1984).
  - [13] M. Hines and J.J. Blum, *Biophys. J.* **47** 705-708 (1985).
  - [14] S. Camalet and F. Jülicher, *New. J. Phys.* **2** 24 (2000).
  - [15] A. Hilfinger and F. Julicher, *Phys. Biol* **5** 016003 (12pp) (2008).
  - [16] B. Schutz, **Geometrical Methods of Mathematical Physics**, Cambridge Univ. Press, 1980.

- [17] T. Frankel, **The Geometry of Physics**, Cambridge Univ. Press, 1997.
- [18] S. Asakura, *Advances in Biophysics* **1** 99-155 (1970).
- [19] S.V. Srigiriraju and T.R. Powers, *Phys. Rev. E.* **73** 011902 (2006).

## Figure Captions

Fig. 1: Schematic cross-section of a cilium showing the 9+2 arrangement of microtubules (dots) and microtubule doublets (double dots), the radial spokes (solid) and the dynein arms (dotted).

Fig. 2: Under the ciliary constraints, the filaments in the neighborhood of a given filament twist about it in a way that is determined by the geometry of the given filament as a space curve (the displacement vector between the filaments is parallel transported along the given filament). The above 9+2 cilium, which is assumed to have taken a helical shape with curvature  $\kappa = 1$  and torsion  $\tau = 2$ , is shown in cross-section as it intersects a plane containing the helix axis. It twists by about  $38^\circ$  on each turn.

Fig. 3: In a twist transition the microtubules shear along each other, but do not generate bend, i.e., the cylinder remains straight. Such a motion violates the ciliary constraints. It may be possible in a 9+0 axoneme, lacking the central 2 microtubules, but not in a 9+2 axoneme, in which the central microtubules enforce the ciliary constraints. The center of the cylinder is deliberately shown empty here.

Fig. 4: In the skew coordinates  $(x,y)$  the distance between  $(0,0)$  and  $(0,1)$  is correctly given as  $\sqrt{1+S^2}$  by the metric tensor of Eq. (7) .

Fig. 5: If filaments are bent into arcs of circles, with arclength  $x$  along the filaments and plane polar coordinates  $(r,\theta)$ , then  $x = r\theta$ , and hence shear strain  $S = -\partial x/\partial r = -\theta = -x/r$  is constant on lines perpendicular to the filaments, a special case of Eq. (29). Also note  $S_x = -1/r$  is the curvature, a special case of Eq. (18). The minus sign is because the curvature vector is opposite to  $e_2 = \partial/\partial r$ .

Fig. 6: The coordinate plane for the surface of the flagellum has lines of constant  $\theta$  that map onto spiraling protofilaments. The coordinate  $x$  is arclength along protofilaments. The dotted line is a line of constant shear strain, determining that the flagellum is a helix of torsion  $\tau$ .